Electronic Supplementary Materials

Polyoxometalate Intercalated MXene with Enhanced Electrochemical Stability

Jun-Jie Zhu[a] and Pedro Gomez-Romero [a,b,*]

[a] Catalan Institute of Nanoscience and Nanotechnology (ICN2), CSIC and BIST, Campus UAB, Bellaterra, 08193 Barcelona, Spain.

[b] Consejo Superior de Investigaciones Científicas (CSIC), Spain

*Author to whom correspondence should be addressed

E-mail address: pedro.gomez@icn2.cat, Tel: +34 937373608, Fax: +34 936917640, ICN2, Campus UAB, 08193 Bellaterra (Barcelona) Spain

Synthesis of quaternary ammonium phosphotungstate derivatives

10 mL of each 30 mM quaternary ammonium (tetramethylammonium hydroxide (TMAOH), tetraethylammonium hydroxide (TEAOH) ,tetrabutylammonium hydroxide (TBAOH), dodecyltrimethylammonium bromide (DTAB) and cetrimonium bromide (CTAB)) solution was added in to 10 mL of 10 mM phosphotungstic acid drop by drop, stirred for 1 h, filtered and dried in vacuum oven at 120 for 6 h. Five types of the quaternary ammonium phosphotungstate saltes (TMAPW12, TEAPW12, TBAPW12, DTAPW12 and CTAPW12) were collected.

Preparation of the pristine PW12 electrode

TEAPW12 powders, carbon superP and PVDF were mixed at a weight ratio of 70:20:10 in a mortar, grinded. A few drops of 1-Methyl-2-pyrrolidone were added into the mixture to form a slurry, coated on aluminum foil, dried at 120°C under vacuum.

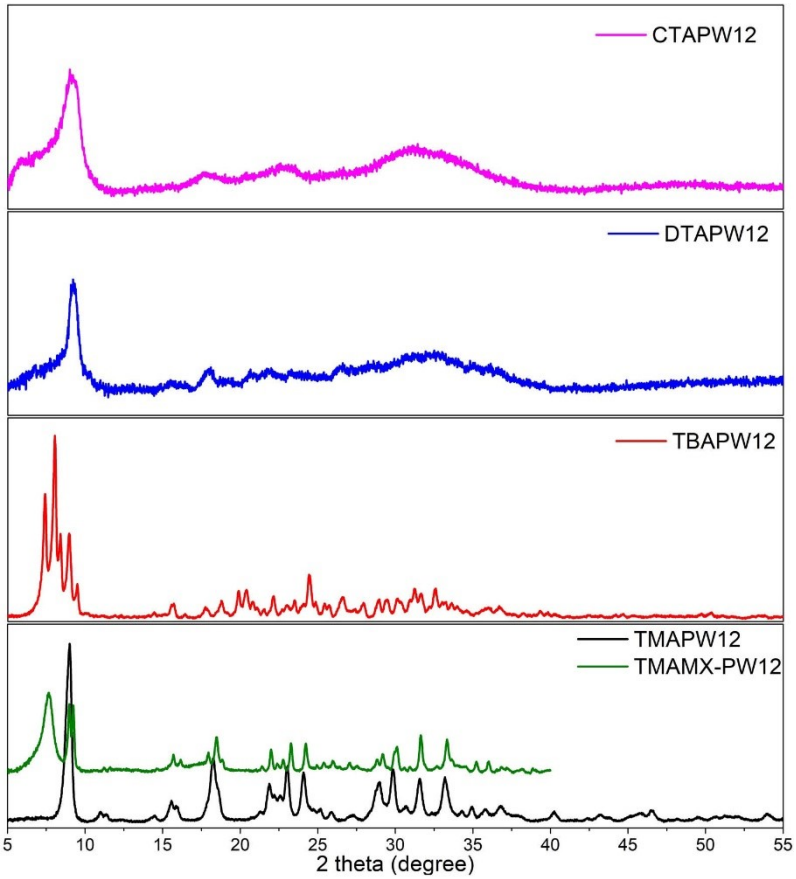

Figure S1. XRD patterns of pristine TMAPW12 (compared with TMAMX-PW12), TBAPW12, DTAPW12 and CTAPW12

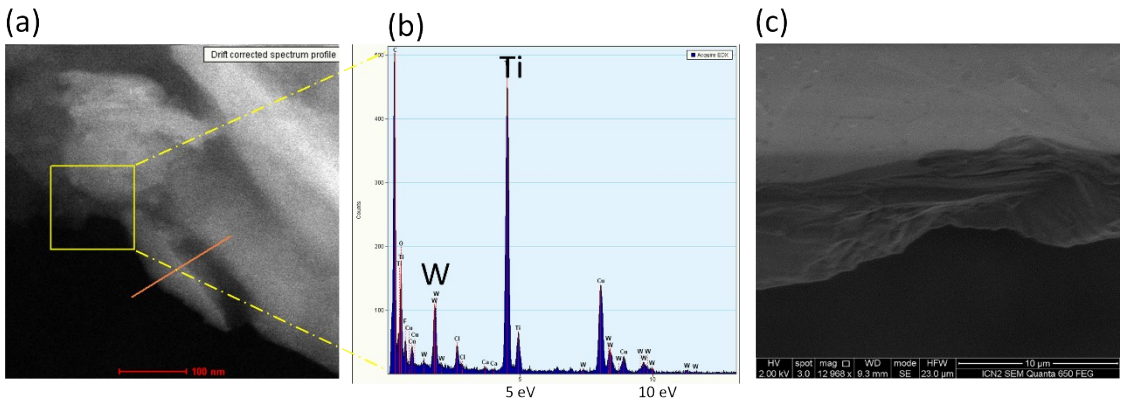

Figure S2. (a) Selected area in the STEM image of CTAMX-PW12 for EDX analysis. (b) Corresponding EDX spectrum. (c) SEM image of pure CTAPW12 which shows a layered structure.

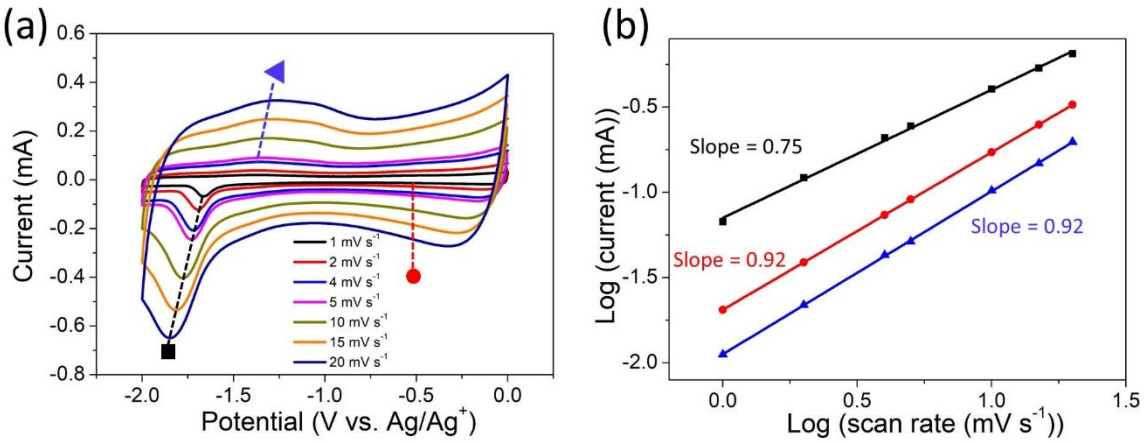

Figure S3. (a) CVs of $Ti_3C_2T_x$ in 1 M TEABF4 in acetonitrile at various scan rates. (b) Linear fitting of log current versus log scan rate plot to determine b values (the slopes) at the peaks (the black and blue) or background rectangle (the red).

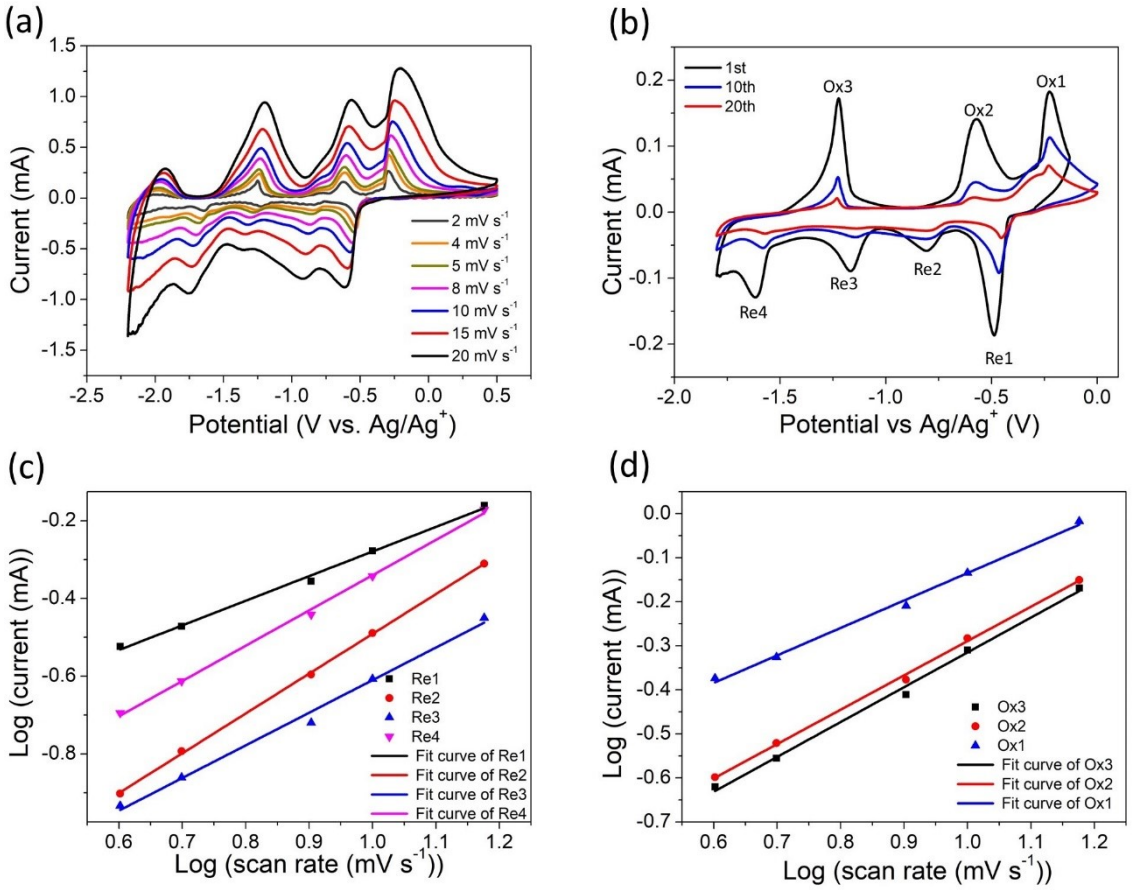

Figure S4. (a) CVs of the pristine PW12 solid electrode at various scan rates in 1 M TEABF4 acetonitrile. (b) CVs of the pristine PW12 solid electrode at 2 mV s^{-1} at the first, 10^{th} and 20^{th} cycles. Linear fitting of log current versus log scan rate plot to determine the b value of (c) reduction peaks and (d) oxidation peaks of PW12 electrode.

Table S1. b-values of the redox peaks of the pristine PW12 solid electrode.

	Re1	Re2	Re3	Re4	Ox1	Ox2	Ox3
crystallized PW12	0.63	1.02	0.84	0.91	0.62	0.78	0.79

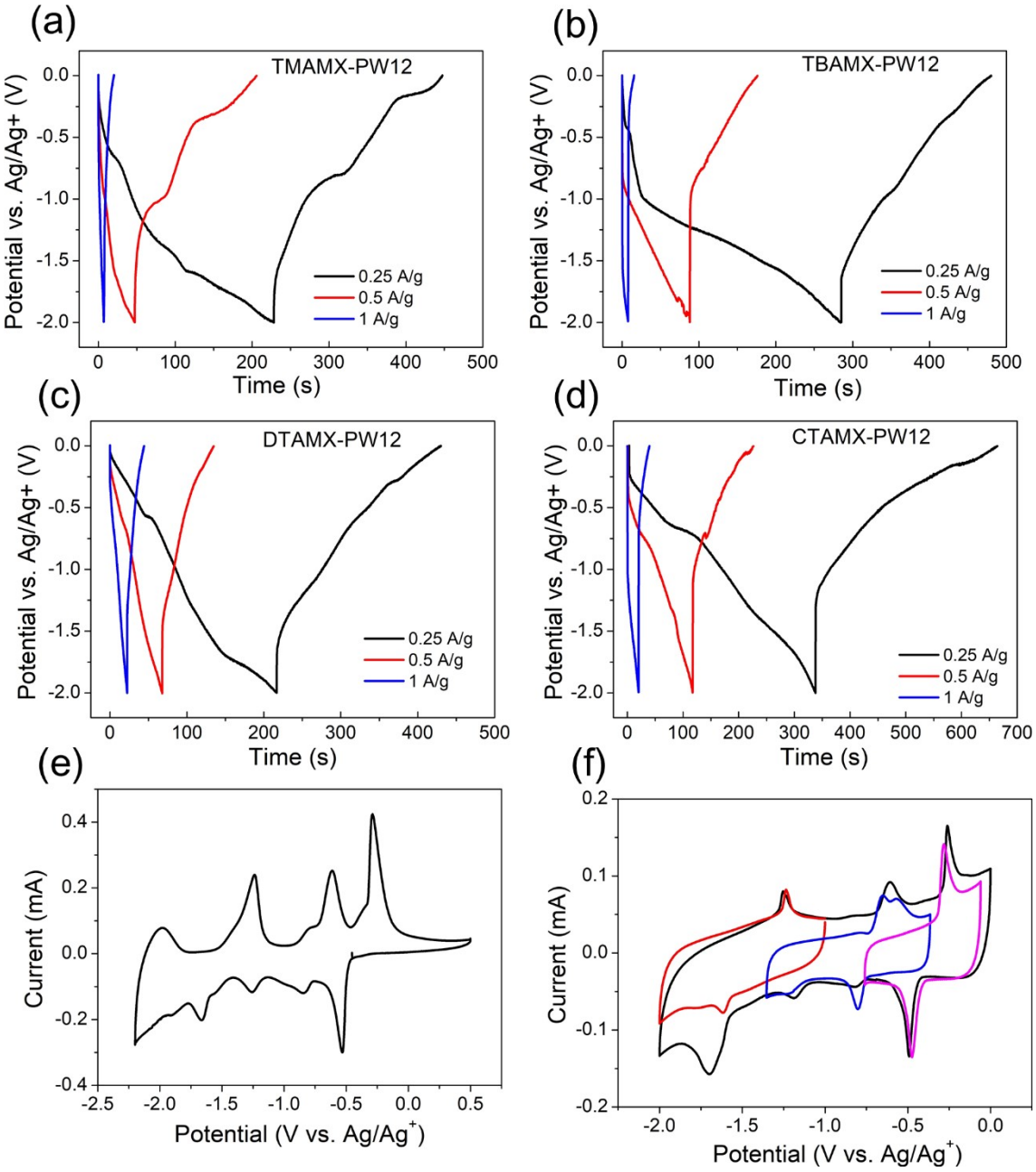

Figure S5. Galvanostatic charge-discharge curves of (a) TMAMX-PW12, (b) TBAMX-PW12, (c) DTAMX-PW12 and (d) CTAMX-PW12 in three-electrode configuration various current densities. (e) CV of pristine solid PW12 electrode (with PVDF binder and carbon black conducting additive) 2 mV s^{-1}. (f) CVs of CTAMX-PW12 at various potential range at 2 mV s^{-1}.

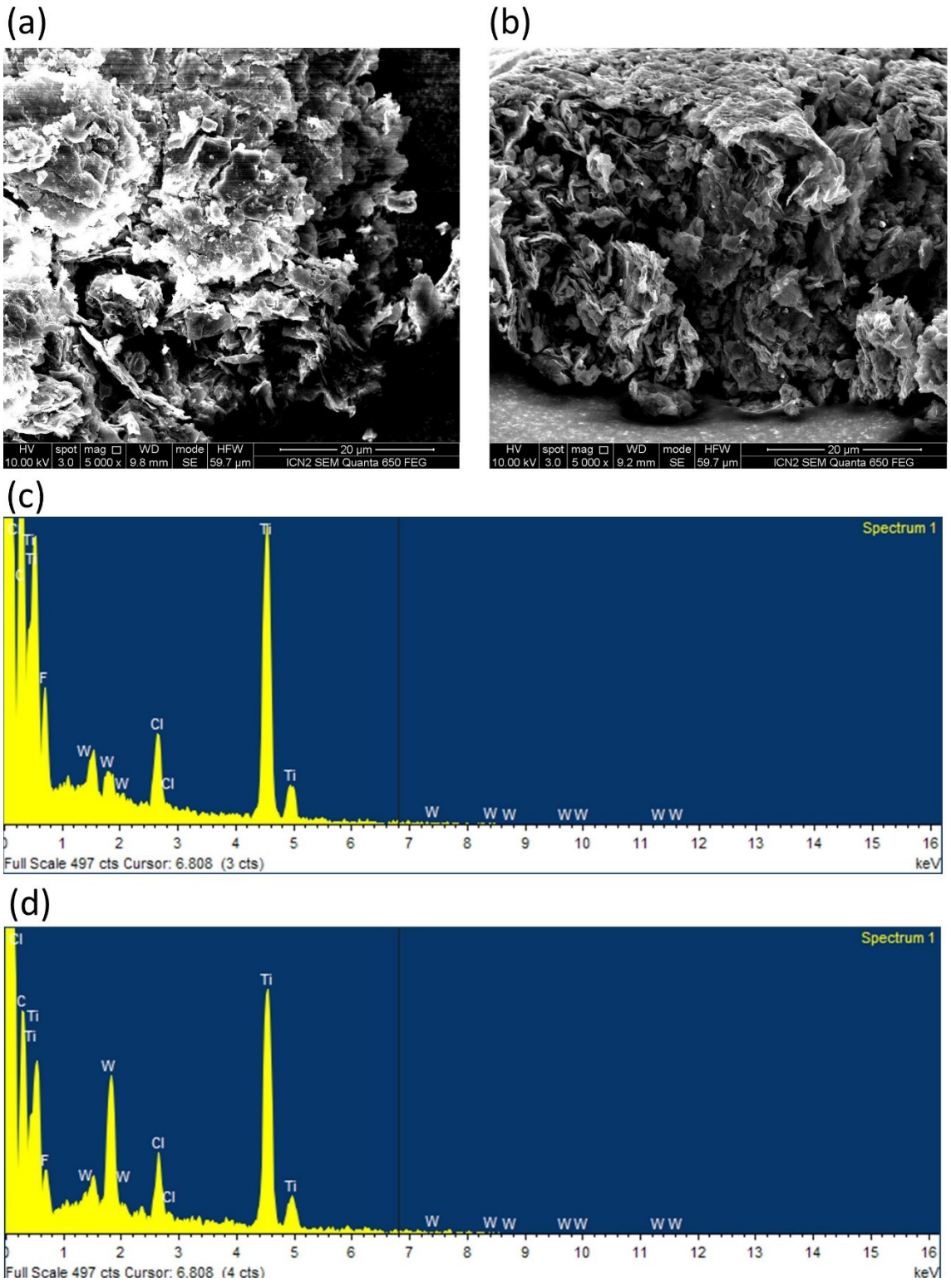

Figure S6. SEM images of cycled (a) TMAMX-PW12 (20 cycles) and (b) CTAMX-PW12 (100 cycles) electrodes. The corresponding EDX spectra of cycled (c) TMAMX-PW12 and (d) CTAMX-PW12.

Table S2. EDX semi-quantitative analysis results of cycled TMAMX-PW12 and CTAMX-PW12

	W wt%	Ti wt%
TMAMX-PW12	3.14	44.00
CTAMX-PW12	12.88	39.11

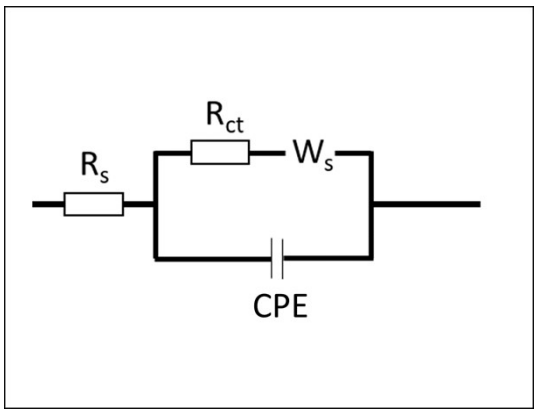

Fig. S7 Equivalent circuit for fitting impedance spectra.

Table S3 Fitting results of impedance sprctra

		R_s/Ω	R_{ct}/Ω	W_s-R/Ω	W_s-T/s	W_s-P	Q/F $s^{(a-1)}$	a
TMAMX-PW12	Fresh	1.34	86.26	81.10	0.13	0.91	4.08E-06	0.94
	Cycled	1.98	142.20	110.20	0.55	0.84	7.00E-06	0.92
TBAMX-PW12	Fresh	1.37	86.48	94.98	0.45	0.90	9.72E-06	0.86
	Cycled	7.30	130.80	114.80	0.65	0.85	1.22E-05	0.88
CTAMX-PW12	Fresh	1.80	64.66	43.98	0.27	0.90	4.09E-06	0.93
	Cycled	1.90	104.40	79.39	0.73	0.88	8.07E-06	0.92